

EVALUATING THE EVOLUTION OF PROCESS SPECIFIC DEGRADATION SIGNATURES AROUND IMPACT CRATERS

JOHN A. GRANT

Center for Earth and Planetary Studies, National Air and Space Museum, Smithsonian Institution,
4th and Independence SW, Washington, DC 20560

Summary—The pristine morphologies created during an impact event comprise a template for constraining how various environmental parameters influence the mechanics of crater formation. Identification of pristine morphologies used in defining and/or evaluating models of crater formation can be complicated or precluded, however, by the effects of post-formation degradation. Field and/or remote examination of simple, unglaciated impact craters on the Earth (*e.g.*, Meteor Crater, Arizona, and Roter Kamm crater, Namibia) can yield results that help to define characteristic degradation signatures for use in placing first-order constraints on the number and intensity of processes that have been active. In turn, the presence of a suite of these degradation signatures can be used to define the amount and style of crater degradation that has taken place, thereby providing a tool for possible distinction between pristine versus secondary, post-formation characteristics.

INTRODUCTION

Impact craters on the Earth and other solar system bodies comprise an important database for evaluating the mechanics of crater formation [*e.g.*, 1-5]. Study of the varying morphology of pristine impact craters occurring in a wide range of planetary settings can yield information for use in relating the formation of certain characteristics to the influence of key environmental parameters (*e.g.*, the role of atmospheric density in the formation of ejecta ramparts, see [1-2]). Interpreting possible mechanisms responsible for the evolution of pristine crater morphology can be complicated, however, by the superposition of secondary, post-formational degradation characteristics.

Examination of simple, unglaciated impact craters on the Earth [6-8] helps to define characteristic degradation signatures for use in placing first-order limits on the number and intensity of processes that have been active. In turn, the presence of a suite of these degradation signatures can be used to constrain the amount and style of crater degradation that has taken place, thereby providing a tool for distinguishing pristine versus secondary, post-formation characteristics.

A summary of the field methods used to quantify the degradation history of Meteor Crater, Arizona [*e.g.*, 6, 9], and Roter Kamm crater, Namibia [8] is followed by presentation of the results from field and remote analysis of other crater structures. These results, in turn, are used to develop a first-order sequence for crater degradation by several processes.

DEGRADATION STATE OF METEOR CRATER, ARIZONA

Meteor Crater, Arizona ($35^{\circ}1'N$, $111^{\circ}1'W$, Fig. 1), has long been recognized as one of the best preserved, naturally formed impact craters on the Earth [e.g., 10-14]. The 1.2 km in diameter crater was formed into nearly flat-lying sedimentary target rocks [10] ~50,000 Ka [15, 16] and preserves a ~300 m wide raised-rim reaching 30-60 m above the level of the surrounding plain. Nevertheless, a comprehensive, quantitative assessment of crater degradation occurring since formation has only recently been completed [6, 9].



Fig. 1. Air photo of the relatively pristine 1.2 km in diameter, 50,000 year old [15, 16] Meteor Crater in north central Arizona ($35^{\circ}1'N$, $111^{\circ}1'W$). View is from the east towards the west. The crater was formed into flat-lying sedimentary rocks and has not been modified by glacial activity.

As summarized from Grant and Schultz [6, 7, 9], traditional field and depositional environment mapping together with remote investigations with a ground penetrating radar (GPR) yield results that help to constrain post-formation crater degradation. Specifically, estimates of the amount of erosion responsible for modification of the continuous ejecta surrounding the crater were based upon: A) evaluation of surface vs. sub-surface concentration of coarse fragments (>4 mm in diameter) created by erosional transport of surface fines; B) the volume of erosionally transported sediments contained within a semi-enclosed drainage basin on the western flank of the crater; and C) the radial extent of preserved ejecta as delineated using a GPR. Evaluation of surface coarsening was based upon grain size analysis of more than 100 samples collected mostly in surface (<10 cm depth) and subsurface (>30 cm depth) pairs and included corrections for possible ambiguities arising from eolian deposition, weathering, and surface wash. Results reveal that *in situ*, pristine ejecta grain size properties are relatively uniform and that low relief surfaces have been subjected to mostly vertical denudation. The volume of sediments within the semi-enclosed depositional basin was constrained by field mapping, excavation, and ground penetrating radar. The total calculated sediment volume includes corrections for possible sediment losses or gains related to more regional-scale alluvial, mass-wasting, and/or eolian activity. Efforts demonstrate that the basin is occupied largely by sediments derived from erosion of ejecta from

intrabasin surfaces and subsequent redistribution into local alluvial, colluvial, and eolian sinks/deposits. Finally, an impulse GPR configured with 500 MHz and 100 MHz transducers was deployed along radial and circumferential transects crossing the medial and distal portion of the ejecta. These data confirm that much of the low relief topography on the distal ejecta surface is created by draping over buried, pre-crater topography typical of that on exposed regional surfaces and that the true extent of the ejecta is often masked by minor accumulations of alluvium and/or colluvium (generally less than 50-100 cm thick).

Each of the approaches outlined yields an independent, but similar estimate of the amount of vertical denudation affecting the ejecta and indicate that much of the crater exterior beyond the immediate near-rim has experienced an average of ~1m or less erosion [6, 7, 9]. Slightly greater degradation of up to 10-15 m affected the higher relief near-rim areas (within ~100-200 m of the rim-crest) and the interior walls [6, 9, 13, 14] and is responsible for increasing the diameter of the vertically undulating rim-crest by 2.5%.

As reported in Grant and Schultz [6, 7], the volume of deposits within the various depositional sinks surrounding the crater confirm that primary degradation was accomplished by alluvial/colluvial and lesser eolian activity. Secondary deflation of fine sediment from these alluvial/colluvial deposits, however, coupled with primary deflation of small ejecta fragments accounts for redistribution of up to 2/3 of all sediment eroded around the crater.

As might be expected, the signatures associated with the limited overall denudation of the crater exterior are subtle (*e.g.*, crater flank incisement is generally less than 5 m) and difficult to detect remotely using data possessing resolution lower than ~1-2 m/pixel (*e.g.*, see Fig. 1). By contrast, the steep interior walls of the crater (30⁰-90⁰ slopes) reflect active backwasting and alluvial processes. Resultant infilling, accompanied by some eolian deposition, buries the original crater floor beneath ~30 m of fill [11]. Signatures associated with degradation of the crater interior include walls that remain sloped at or above the angle of repose and incised debris chutes that are detectable in images possessing a resolution of ~30 m/pixel or better.

The conclusion that Meteor Crater retains a remarkably pristine form [6, 9] is consistent with the results of alternate studies [17, 18] and requires that nearly all of the subtle topography associated with the continuous ejecta deposit at Meteor Crater is pristine, thereby reflecting the influence of conditions present when the crater formed. Such information is invaluable for investigators attempting to relate various aspects of crater formation models to observational field data [*e.g.*, 4, 19, 20]. For example, the distribution of several distal ejecta lobes superposing a low butte ~2.0R north of the crater must be pristine and do not reflect local differences in erosion intensity. Hence, their occurrence can be used to help constrain processes of distal ejecta emplacement [4].

DEGRADATION STATE OF ROTER KAMM CRATER, NAMIBIA

The Roter Kamm impact crater in Namibia (27⁰46'S; 16⁰18'E) is ~2.5 km in diameter (Fig. 2) and was formed into crystalline target rocks [21] approximately 3.7 Ma ago [22]. Roter Kamm retains a raised-rim extending 40 to 90 m above the surface. Eolian sands associated with an up to 10 m thick regional sand sheet [21, 23] bury all but the highest portions of the rim and are responsible for ~500 m of fill within the crater [8, 24]. Sediments associated with eolian infilling limit the present depth of the crater to ~50 meters below the surrounding plain. An impact origin for Roter Kamm was first proposed by Dietz [25] and Fudali [24] and confirmed by Miller and Reimold [26], Reimold and Miller [27], and Reimold *et al.* [28, 29]. Evaluation of the preservation state of the crater was more recently accomplished via interpretation of topographic information, GPR data, and analysis of sediment samples from around the crater [8].



Fig. 2. View of a portion of the exposed rim and interior of the 2.5 km in diameter, ~3.7 million year old [22] Roter Kamm crater in the Namib Desert, Namibia ($27^{\circ}46'S$; $16^{\circ}18'E$). View is from the north rim-crest towards the southeast and illustrates the subdued, incised form of the exposed upper rim-crest and extensive infilling of the crater by sediments associated with the regional sand sheet. The crater was formed into mostly crystalline rocks and has not been modified by glacial activity.

As summarized from Grant *et al.* [8], topographic data reveal that Roter Kamm presents a subdued form relative to Meteor Crater. Gradients on the exposed interior walls of the crater range between 8° - 22° and the rim presents a broader, more rounded expression that is locally incised by up to 30 m. Interpretation of topographic information was assisted by collection of GPR data (using an impulse GPR system configured with 500 MHz and 100 MHz transducers) from within and around the crater along transects totaling 15 km in length. These GPR data typically delineate reflections beneath the sand sheet to depths of 3-5 m and help define the nature and extent of near-surface stratigraphic and/or pedogenic horizons. GPR data also assisted in identifying locations where ground truth and samples were obtained for evaluation of grain size and textural properties (*e.g.*, shape and sorting).

Exposed portions of the crater rim are relatively limited in areal extent and are characterized by heavily fractured bedrock. GPR data from along the upper interior wall of the crater defines a reflection corresponding to the crater wall and/or alluvium mantling the crater wall that can be traced beneath the sand fill and confirm that slopes on exposed wall surfaces persist beneath at least the upper portions of the fill. By contrast, GPR and sedimentologic data collected along transects descending the exterior flank of the crater distinguish a deposit beneath the sand sheet whose radar and sedimentologic properties are most consistent with an origin related to alluvial transport from higher on the rim (Fig. 3). The thickness of this alluvium exceeds the penetration depth of the GPR.

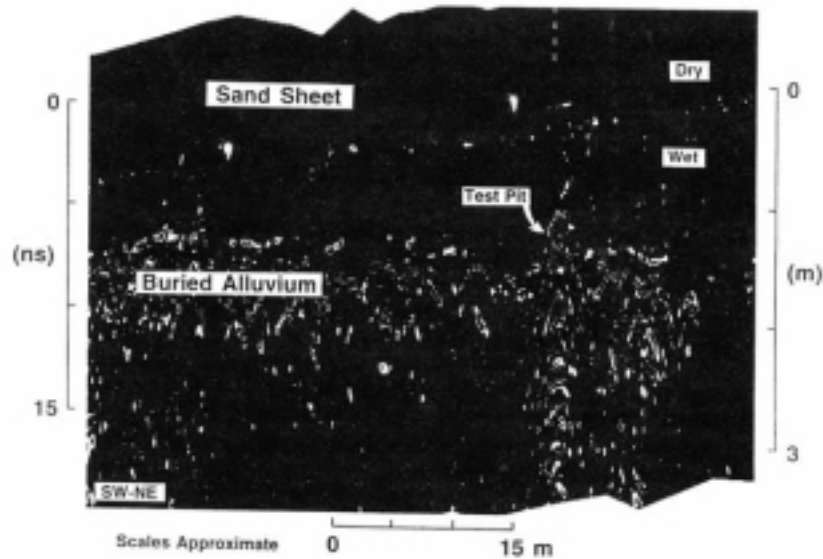


Fig. 3. Portion of a ground penetrating radar (GPR) transect completed down the eastern outer flank of Roter Kamm. Data delineate a reflection beneath the regional sand sheet sediments corresponding to the top of extensive alluvium whose thickness exceeds the penetration depth of the GPR. Comparable accumulations of alluvium occur on at least the east and south flanks of the crater [8]. The reflection within the sand sheet marks the transition from dry to damp sand and highlights the sensitivity of the GPR to changing moisture.

With only one exception, all GPR reflections delineated beyond the base of the exterior flank of the crater are created by nodular to massive pedogenic calcrete horizons and/or bedrock. An isolated GPR reflection identified on a slightly elevated surface 2.4 crater radii north of the rim, however, corresponds to a deposit of coarse, unsorted, angular-to-subangular fragments that are supported in a finer-grained matrix. These fragments are coarser, more poorly sorted, and more angular than the fragments comprising either the alluvial deposits on the crater flank and the pedogenic calcretes noted above. Moreover, grain mounts of constituent fragments display abundant planar deformation features and confirm their involvement in the impact event. On the basis of these attributes, the deposit is identified as preserved ejecta that have been modified by colluvial and pedogenic processes, but remained largely *in situ*. The isolated deposit comprises the only ejecta identified to date at Roter Kamm.

Interestingly, the properties of the Roter Kamm ejecta [8] are remarkably similar to those at Meteor Crater [6] for the range of sizes evaluated despite differences in involved target rocks. The moderate to high rates of surface infiltration and hydraulic conductivity indicated by these ejecta size distributions [30] likely plays an important role in controlling the amount of runoff on the ejecta that is available for development of fluvial degradation signatures.

Topographic, GPR, and sedimentologic data from in and around Roter Kamm assist in distinguishing deposits preserving at least a partial record of crater degradation [8]. Although well-preserved from a structural standpoint, these data reveal that erosion accounts for nearly complete removal of the continuous ejecta deposit, approaches 50 m in higher relief near-rim areas, and accounts for an increase in the diameter of the crater by ~10%.

As discussed in Grant *et al.* [8], several factors indicate that degradation of ejecta at Roter Kamm resulted from mostly fluvial and lesser eolian activity: A) the broad extent and sedimentologic properties of alluvium within and around the crater; B) deep incisement of the crater rim; and C) nearly complete redistribution of coarse ejecta fragments that are too large for transport by eolian processes.

Stratigraphic and climatic data [31, 32] reveal that alluvial activity would have been most important during the pre-Pleistocene history of the crater and was followed by more recent eolian modification associated with arrival of the regional sand sheet. It is likely that mass wasting played an important role in early degradation of the crater interior when the gradients on the walls were much higher than at present [*e.g.*, see 14, 20, 33]. Any deposits associated with such activity, however, remain undetected. The low slope presently characterizing the crater walls together with the inability to detect these deposits through thick overlying alluvium and eolian fill imply significant mass wasting was mostly confined to the earliest history of crater modification.

Significant denudation at Roter Kamm has been accomplished by mass wasting, fluvial, and eolian activity whose relative importance likely varied in chronological order [8]. Significant mass-wasting probably characterized early back-wasting of the crater wall and colluvial redistribution of ejecta fragments, but became less important as wall slopes were reduced by runoff. Fluvial activity accounts for most of the erosion at the crater and has accomplished nearly complete removal of the continuous ejecta deposit. Ongoing eolian redistribution of sediments associated with the regional sand sheet effectively mask many of the older mass-wasting and fluvial signatures evolved at the crater. Nevertheless, diagnostic evidence of the importance of fluvial processes persists in the form of a deeply incised rim and low wall slopes. The absence of preserved ejecta and the modified form of Roter Kamm suggest that cratering models would be of limited usefulness as tools for understanding anything more than the first-order formation mechanics.

The preceding discussion of Meteor Crater and Roter Kamm serve to illustrate the ability to constrain the amount and processes of degradation affecting impact craters. Results from Meteor Crater and Roter Kamm together with data collected from field and/or remote evaluation of other simple, unglaciated craters permit definition of a general evolutionary sequence for terrestrial crater degradation.

A FIRST-ORDER DEGRADATION SEQUENCE FOR SIMPLE TERRESTRIAL CRATERS

The degradation state of several other terrestrial craters/structures has also been investigated. This ongoing effort includes field work at the Odessa Craters ($31^{\circ}45'N$, $102^{\circ}29'W$), Texas [34] and the results of remote investigation of Lonar Crater ($20^{\circ}N$, $76.5^{\circ}E$) and the Ramgarh Structure ($25^{\circ}20'N$, $76^{\circ}37'E$), India, the Pretoria Saltpan ($25^{\circ}34'S$, $28^{\circ}5'E$), South Africa, and Talemzane Crater ($33.3^{\circ}N$, $4.0^{\circ}E$), Algeria [7, 35]. All of these craters are formed into nearly flat-lying sedimentary and/or volcanic and/or crystalline rocks.

The Odessa Craters consist of a main depression that is ~ 0.17 km diameter and several smaller depressions that were formed simultaneously $\sim 25,000$ Ka [36, 37]. Lonar Crater is 1.8 km in diameter and was formed 62 Ka [38, 39], whereas the Ramgarh structure is 4.1 km in diameter and of unknown age [40]. The Pretoria Saltpan is 1.13 km in diameter and approximately 200 Ka [41]. Talemzane Crater is 1.75 km in diameter and formed sometime between 0.5-3.0 Ma [42, 43]. Comparative analysis of the degradation signatures at these structures permits definition of a sequence of diagnostic morphologic characteristics that may accompany advancing crater degradation by fluvial, mass wasting, and eolian processes (see Grant and Schultz [7, 8, 35]).

For example, analysis of evolved degradation signatures reveals that mass wasting on interior crater walls is typically most important during early crater modification. Mass-wasting is then superseded by fluvial activity as unconsolidated and fractured debris is shed from the crater walls and slopes are reduced to and then below the angle of repose (Fig. 4). Modification of the exterior of the craters by mass wasting is limited primarily to local redistribution of fragments by colluviation. Once important, fluvial degradation of crater interiors proceeds rapidly as a result of the initially higher slopes and low

infiltration rates characteristic of the crater walls. Resultant high stream power within the craters leads to rapidly evolving systems that initially incise increasingly inactive debris chutes and quickly erode headward to first notch and then incise the crater rim (Fig. 4). Eventually, the interior drainages breach the rim and begin to capture the headward reaches of basins draining the crater exterior, thereby leading to further crater infilling, steady reduction in wall slopes, and crater enlargement (Fig. 4). By contrast, the drainages evolving outside of the craters steadily increase in size and density as they strip most or all of the continuous ejecta, but they do not achieve the scale of the systems within the craters. One factor important in controlling the scale of exterior drainages is the high infiltration rate and hydraulic conductivity within the ejecta that impedes runoff. The larger scale and increasing density of the interior systems (Fig. 4) means that they are more readily detected and measured than the smaller scale systems evolving around the craters. Wall slopes, drainage density, and drainage scale (or degree of incisement) all change systematically with increasing fluvial degradation and are relatively easy to measure. These parameters, therefore, are considered to be the least ambiguous indicators of increasing stages of fluvial degradation. Eolian erosion of craters is mostly limited to primary and secondary deflation of fines from exposed ejecta, colluvial, and alluvial surfaces, and development of small-scale ventifacts and yardangs. Although potentially responsible for transport of significant material derived from erosion of ejecta by a range of processes, primary eolian erosion is typically subordinate to modification by alternate processes. Eolian erosion may be briefly more important for a short period following crater formation when surfaces are not yet stabilized by the effects of alternate, more competent processes. Significant eolian deposition can be responsible for considerable crater infilling and masking of many signatures evolved by the action of alternate processes. Nevertheless, the higher relief associated with crater rims inhibits burial and frequently enables measure of wall slope, rim incisement, and drainage density to assess the degree of fluvial modification.

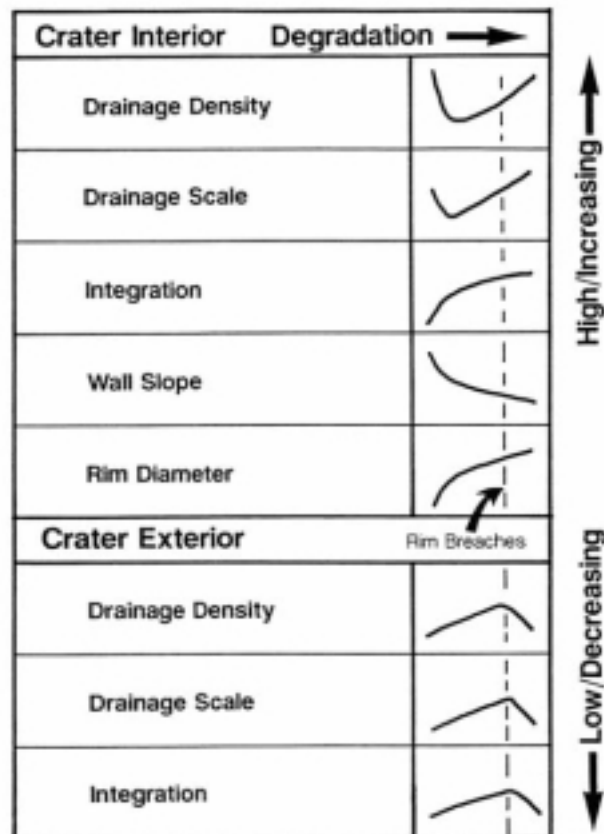


Fig. 4. Qualitative illustration of characteristic signatures associated with advancing fluvial degradation of simple, unglaciated impact craters on the Earth.

SUMMARY

Based on the preceding discussion, the craters/structures examined to date can be placed in order of increasing degradation state (Fig. 5): Meteor Crater, Lonar Crater, Ramgarh Structure, Pretoria Saltpan, Odessa, Talemzane, and Roter Kamm. Although largely qualitative, the first order sequence presented in figure 5 does permit assignment of processes most responsible for modification and, in many instances, places broad limits on the scale and degree to which primary formational characteristics of impact craters can be resolved. Such information can also be useful for evaluating the amount and process(es) of degradation operating on other planets.

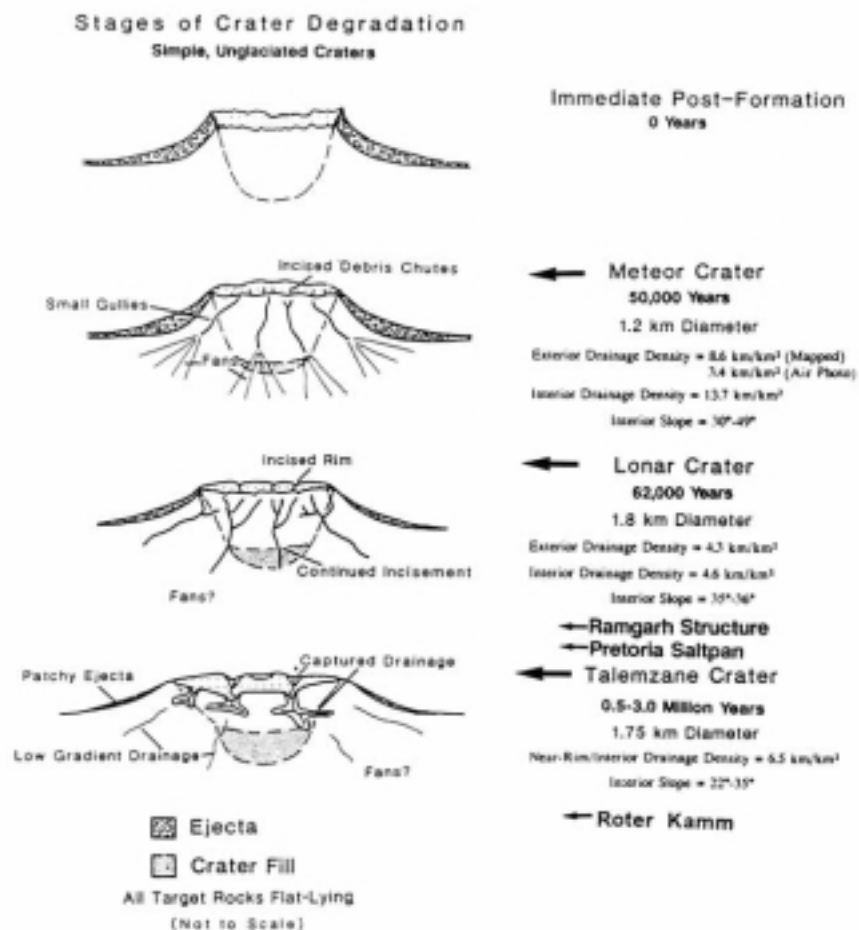


Fig. 5. Graphic illustration of a first-order degradation sequence for simple, unglaciated impact craters on the Earth. The relative degradation state of craters discussed in the text is indicated along with characteristic variations in drainage density, scale, and interior wall slope. Further definition of signatures evolved around other terrestrial craters should help to place more quantitative limits on the degradation stages, thereby enabling better resolution of pristine versus degradational characteristics associated with craters on the Earth and planets.

For example, Martian impact craters display a tremendous range in morphology. Some (Fig. 6) reveal evidence of extensive crater wall incisement, rim breaching, and reduction of wall slopes below the angle of repose [e.g. 44]. Although the size/type of the Martian crater illustrated in Figure 6 (complex versus simple) and associated geologic and climatic setting may not be directly analogous to those discussed for the terrestrial craters examined so far, cited degradation characteristics appear indicative of considerable fluvial modification. Refinement of terrestrial crater degradation sequences may eventually permit more quantitative evaluation of this and other Martian craters and help to confirm the possible role of running water in crater degradation. Further, results might assist in assessment of the amount and source of any water involved in the development of observed features (e.g., runoff vs. groundwater sapping vs. mass wasting or other source, see [45-49]).

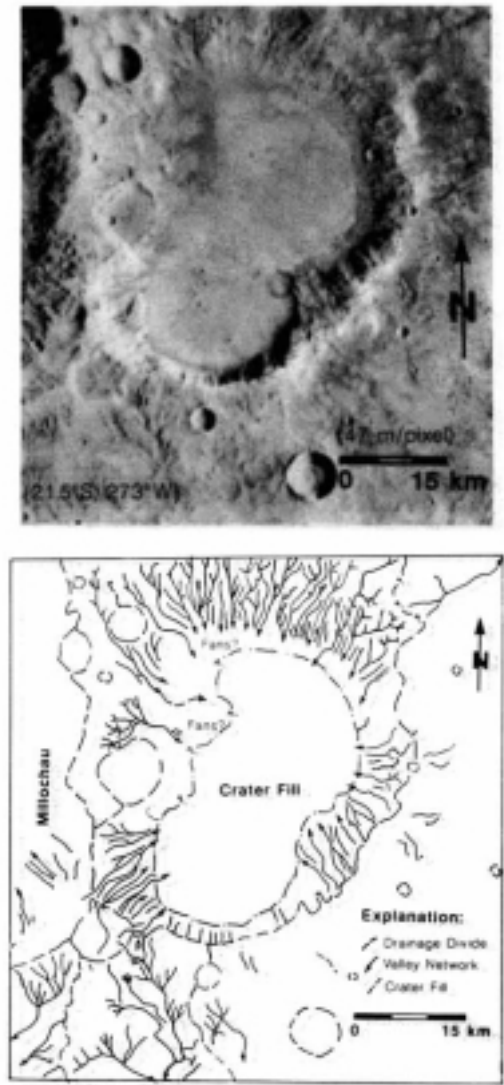


Fig. 6. Viking Orbiter image and geomorphic map of a degraded impact crater located east of Crater Millochau in Terra Tyrrhena, Mars [44]. While perhaps not directly analogous to the terrestrial craters discussed, the Martian crater displays an incised rim, low sloping walls, and significant infilling that may reflect modification by running water. Better definition of the characteristic signatures associated with increasing degradation by mass-wasting, fluvial, and eolian processes could eventually enable constraint of the amount and source of any water involved in development of the observed morphology.

Knowledge of degradation state and the history of active erosional processes can enable distinction between pristine and degradational characteristics of craters on the Earth and planets, thereby assisting in definition of ground truth for efforts geared towards modeling crater formation and understanding the influence of environmental variables on resultant crater morphology.

Acknowledgement—Constructive comments made by two anonymous reviewers are much appreciated. Thanks to Pete Schultz, Chris Koeberl, Mary Grant, and Nancy Grant. This effort was supported in part by NASA Grant NAG5-4157 to John Grant and NAG5-3877 to Pete Schultz.

REFERENCES

1. P.H. Schultz, Atmospheric effects on cratering efficiency. *J. Geophys. Res.*, **97**, 975-1005 (1992).
2. P.H. Schultz, Atmospheric effects on ejecta emplacement. *J. Geophys. Res.*, **97**, 11,623-11,662 (1992).
3. P.H. Schultz and D.E. Gault, Atmospheric effects on Martian ejecta emplacement. *J. Geophys. Res.*, **84**(B13), 7669-7687 (1979).
4. P.H. Schultz and J.A. Grant, Styles of ejecta emplacement, Meteor Crater. *Lunar and Planet. Sci. XX*, pp. 972-973, LPI, Houston, TX, March (1989).
5. O.S Barnouin-Jha and P.H. Schultz, Ejecta entertainment by impact-generated vortices: Theory and experiments. *J. Geophys. Res.*, **101**, 21,099-21,116 (1986).
6. J.A. Grant and P.H. Schultz, Erosion of Ejecta at Meteor Crater, Arizona. *J. Geophys. Res.*, **98**, 15,033-15,047 (1993).
7. J.A. Grant and P.H. Schultz, Degradation of selected terrestrial and Martian impact craters. *J. Geophys. Res.*, **98**, 11,025-11,042 (1993).
8. J.A. Grant, C. Koeberl, W.U. Reimold, and P.H. Schultz, Gradation of the Roter Kamm impact Crater, Namibia. *J. Geophys. Res.*, **102**, 16,327-16,388 (1997).
9. J.A. Grant and P.H. Schultz, Erosion of ejecta at Meteor Crater: Constraints from ground penetrating radar. *Proc. 5th Int. Conf. on Ground Penetrating Radar (GPR '94)*, pp. 789-803, June 12-16, 1994, Kitchener, Ontario, Canada, June (1994).
10. E.M. Shoemaker and S.E. Kieffer, *Guidebook to the geology of Meteor Crater, Arizona*. Arizona State Univ. Cent. Meteorite Stud. Pub. **17**, Tempe, AZ, 66pp. (1974).
11. E.M. Shoemaker, *Impact mechanics at Meteor Crater, Arizona*. Ph.D. Dissertation, Princeton Univ., Princeton, NJ, 55pp. (1960).
12. E.M. Shoemaker, Meteor Crater, Arizona. In *Centennial Field Guide, v. 2, Rocky Mountain Section of the Geological Society of America* (edited by S.S. Beus), pp. 399-404, Geol. Soc. Am., Boulder, CO (1987).
13. D.J. Roddy, J.M. Boyce, G.W. Colton, and A.L. Dial, Jr., Meteor Crater, Arizona, rim drilling with thickness, structural uplift, diameter, depth volume, and mass-balance calculations. *Proc. 6th Lunar and Planet. Sci. Conf.*, pp. 2621-2644, LPI, Houston, TX (1975).
14. D.J. Roddy, Pre-impact geologic conditions, physical properties, energy calculations, meteorite and initial crater dimensions and orientations of joints, faults, and walls at Meteor Crater, Arizona. *Proc. 9th Lunar and Planet. Sci. Conf.*, pp. 3891-3930, LPI, Houston, TX (1978).
15. S.R. Sutton, Thermoluminescence measurements on shock-metamorphosed sandstone and dolomite from Meteor Crater, Arizona: 2. Thermoluminescence age of Meteor Crater. *J. Geophys. Res.*, **90**(B5), 3690-3700 (1985).
16. K. Nishiizumi, C.P. Kohl, E.M. Shoemaker, J.R. Arnold, D. Lal, J. Klein, D. Fink, and R. Middleton, In Situ Be¹⁰-Al²⁶ exposure ages at Meteor Crater, Arizona. *Lunar and Planet. Sci. XX*, pp. 792-793, LPI, Houston, TX (1989).
17. J.A. Pilon, R.A.F. Grieve, and V.L. Sharpton, The subsurface character of Meteor Crater, Arizona, as determined by ground-probing radar. *J. Geophys. Res.*, **96**, 15,563-15,576 (1991).
18. F.M. Phillips, M.G. Zreda, S.S. Smith, D. Elmore, P.W. Kubik, R.I. Dorn, and D.J. Roddy, Age and geomorphic history of Meteor Crater, Arizona, from cosmogenic ³⁶Cl and ¹⁴C in rock varnish. *Geochim. Cosmochim. Acta*, **55**, 2695-2698 (1991).
19. D.J. Roddy, S.H. Schuster, K.N. Kreyenhagen, and D.L. Orphal, Computer code simulations of the formation of Meteor Crater, Arizona: Calculations MC-1 and MC-2. *Proc. 11th Lunar and Planet. Sci. Conf.*, pp. 2275-2308, LPI, Houston, TX (1980).
20. J.B. Garvin, J.L., Bufton, B.A., Campbell, and S.H. Zisk, Terrain analysis of Meteor Crater ejecta blanket. *Lunar and Planet. Sci. XX*, pp. 333-334, LPI, Houston, TX (1989).

21. R.McG. Miller and K.E.L. Schalk, *Namibia Geological Map*. Geological Survey of Namibia, Windhoek, Namibia (1980).
22. C. Koeberl, J.B. Hartung, M.J. Kunk, J. Klein, J.I. Matsuda, K. Nagao, W.U. Reimold, and D. Storzer, The age of the Roter Kamm impact crater, Namibia: Constraints from ^{40}Ar - ^{39}Ar , K-Ar, Rb-Sr, fission-track, and ^{10}Be - ^{26}Al studies. *Meteoritics*, **28**, 204-212 (1993).
23. E.D. McKee, Sedimentary Structures in Dunes of the Namib Desert, South West Africa. *Geol. Soc. Am. Spec. Paper* **188**, Geol. Soc. Am., Boulder, CO, 64pp. (1982).
24. R.F. Fudali, Roter Kamm: Evidence for an impact origin. *Meteoritics*, **8**, 245-257 (1973).
25. R.S. Dietz, Roter Kamm, Southwest Africa: Probable meteorite crater. *Meteoritics*, **2**, 311-314 (1965).
26. R.McG. Miller and W.U. Reimold, Deformation and shock deformation in rocks from the Roter Kamm crater, SWA/Namibia. *Meteoritics*, **21**, 456-458 (1986).
27. W.U. Reimold and R.McG. Miller, The Roter Kamm impact crater, SWA/Namibia. *Proc. 19th Lunar and Planet. Sci. Conf.*, pp. 711-732, LPI, Houston, TX (1989).
28. W.U. Reimold, R.McG. Miller, R.A.F. Grieve and C. Koeberl, The Roter Kamm impact structure in SWA/Namibia. *Lunar and Planet. Sci. XIX*, pp. 972-973, LPI, Houston, TX (1988).
29. W.U. Reimold, C. Koeberl and J. Bishop, Roter Kamm impact crater, Namibia: Geochemistry of basement rocks and breccias. *Geochim. Cosmochim. Acta*, **58**, 2689-2710 (1994).
30. W.K. Summers and P.A. Weber, The relationship of grain-size distribution and hydraulic conductivity - an alternate approach. *Groundwater*, **22**, 474-475 (1984).
31. Cooperative Holocene Mapping Project (COHMAP) Members, Climatic changes of the last 18,000 years: Observations and model simulations. *Science*, **241**, 1043-1052 (1988).
32. P.B. deMenocal, Plio-Pleistocene African climate. *Science*, **270**, 53-59 (1995).
33. R.A.F. Grieve and J.B. Garvin, A geometric model for excavation and modification at terrestrial simple impact craters. *J. Geophys. Res.*, **89**, 11,561-11,572 (1984).
34. J.A. Grant and P.H. Schultz, Characteristics of Ejecta and Alluvial Deposits at Meteor Crater, Arizona and Odessa Craters, Texas: Results from Ground Penetrating Radar. *Lunar and Planet. Sci. XXII*, pp. 481-482, LPI, Houston, TX (1991).
35. J.A. Grant and P.H. Schultz, Gradational Evolution of Young, Simple Impact Craters on the Earth. *Lunar and Planet. Sci. XXII*, pp. 483-484, LPI, Houston, TX (1991).
36. E.H. Sellards and G.L. Evans, *Statement of Progress of Investigation at Odessa Meteor Craters*: Univ. of Texas, Bur. Econ. Geol., 12pp. (1941).
37. G.L. Evans, Investigations at the Odessa meteor craters. *Proc. Geophys. Lab./Lawrence Rad. Lab. Cratering Symp.*, Wash., D.C., March 1961 (edited by M.D. Nordyke), 11pp., Paper D, Univ. Calif. Livermore Rad. Lab. Rept. UCRL-6438, Livermore, CA (1961).
38. K. Fredriksson, A. Dube, D.J. Milton, and M.S. Balasundaram, Lonar lake, India: An impact crater in basalt. *Science*, **180**, 862-864 (1973).
39. R.A.F. Grieve, C.A. Wood, J.B. Garvin, G. McLaughlin, and J.F. McHone, Jr., *Astronaut's Guide to Terrestrial Impact Craters*. LPI Tech Rpt. **88-03**, LPI, Houston, TX, 89pp. (1988)
40. A.V. Murali and K.P. Lulla, Ramgarh Crater, Rajasthan, India: Study of multispectral images obtained by Indian Remote Sensing Satellite (IRS-IA). *Geocarto International*, **7**, 75-80 (1992).
41. W.U. Reimold, C. Koeberl, T.C. Partridge, and S.J. Kerr, Pretoria Saltpan crater: Impact origin confirmed. *Geology*, **20**, 1079-1082 (1992).
42. R. Karpoff, The meteorite crater of Talemzane in southern Algeria. *Meteoritics*, **1**, 31-38 (1963).
43. P. Lambert, J.F. McHone, Jr., R.S. Dietz, and M. Houfani, Impact and impact-like structures in Algeria, Part 1. Four bowl-shaped depressions. *Meteoritics*, **15**, 157-179 (1980).
44. J.A. Grant and P.H. Schultz, Early fluvial degradation in Terra Tyrrhena, Mars: Constraints from styles of crater degradation on the Earth. *Lunar and Planet. Sci. XXV*, pp. 457-458, LPI, Houston, TX (1994).
45. M.H. Carr, *The Surface of Mars*. Yale University Press, New Haven, CT, 232pp. (1981).
46. V.R. Baker, *The Channels of Mars*. University of Texas press, Austin, TX, 198pp. (1982).
47. Mars Channel Working Group, Channels and valleys on Mars. *Geol. Soc. Am. Bull.*, **94**, 1035-1054 (1983).
48. M.H. Carr and F.C. Chuang, Martian drainage densities. *J. Geophys. Res.*, **102**, 9145-9152 (1997).
49. J.A. Grant, 1997, Geologic mapping and drainage basin analysis in Margaritifer Sinus, Mars. *Lunar and Planet. Sci. XXVIII*, pp. 451-452, LPI, Houston, TX (1997).